Design of Multipath Channel Model For Shallow Under Water Acoustic Communication System using QPSK Modulation

A Project report submitted in partial fulfilment of the requirements for the award of the degree of

BACHELOR OF TECHNOLOGY

IN

ELECTRONICS AND COMMUNICATION ENGINEERING

Submitted by

G.Sunil (319126512143)

I.Pushpalatha (319126512149)

K.Shivani (319126512154)

M.Chaitanya (319126512160)

Under the guidance of

Dr.Ch.Padma Sree

Assistant Professor

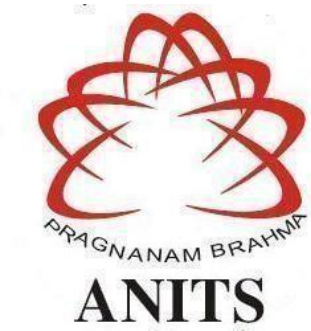

DEPARTMENT OF ELECTRONICS AND COMMUNICATION ENGINEERING

ANIL NEERUKONDA INSTITUTE OF TECHNOLOGY AND SCIENCES

(UGC AUTONOMOUS)

(Permanently Affiliated to AU, Approved by AICTE and Accredited by NBA & NAAC)

Sangivalasa, Bheemili Mandal, Visakhapatnam Dist. (A.P)

2022-2023

DEPARTMENT OF ELECTRONICS AND COMMUNICATION ENGINEERING
ANIL NEERUKONDA INSTITUTE OF TECHNOLOGY AND SCIENCES
(UGC AUTONOMOUS)

(Permanently Affiliated to AU, Approved by AICTE and Accredited by NBA & NAAC with 'A' Grade)

Sangivalasa, Bheemili Mandal, Visakhapatnam Dist.(A.P)

PRAGNANAM BRAHMA

ANITS

CERTIFICATE

This is to certify that the industrial training report entitled " **Design of Multipath Channel Model For Shallow Under Water Acoustic Communication System using QPSK Modulation"** submitted by **G.Sunil (319126512143), I.Pushpalatha (319126512149), K.Shivani (319126512154), M.Chaitanya (319126512160)** in partial fulfillment of the requirements for the award of the degree of **Bachelor of Technology** in **Electronics & Communication Engineering** is a record of bonafide work carried out under my supervision.

Padma 17/4/23

Project Guide

Dr.Ch.Padma Sree
Assistant Professor
Department of ECE
ANITS

Assistant Professor
Department of E.C.E.
Anil Neerukonda
Institute of Technology & Sciences
Sangivalasa, Visakhapatnam-531 162

Head of the Department

Prof.B.Jagadeesh
Professor & HOD
Department of ECE
ANITS

Head of the Department
Department of E C E
Anil Neerukonda Institute of Technology & Sciences
Sangivalasa - 531 162

ACKNOWLEDGEMENT

We would like to express our deep gratitude to our project guide **Dr.Ch.Padma Sree** Assistant Professor, Department of Electronics and Communication Engineering, ANITS, for his guidance with unsurpassed knowledge and immense encouragement.

We are grateful to **Prof. B. Jagadeesh**, Head of the Department, Electronics and Communication Engineering, for providing us with the required facilities for the completion of the project work.

We are very much thankful to the **Principal and Management, ANITS, Sangivalasa,** for their encouragement and cooperation to carry out this work.We express our thanks to all **teaching faculty** of Department of ECE, whose suggestions during reviews helped us in accomplishment of our project. We would like to thank **all non teaching staff** of the Department of ECE, ANITS for providing great assistance in accomplishment of our project.

We would like to thank our parents, friends, and classmates for their encouragement throughout our project period. At last but not the least, we thank everyone for supporting us directly or indirectly in completing this project successfully.

PROJECT STUDENTS

G.Sunil (319126512143)

I.Pushpalatha (319126512149)

K.Shivani (319126512154)

M.Chaitanya (319126512160)

ABSTRACT

Many studies have recently concentrated on the development of dependable underwater audio communication systems. Based on the depth of the water, Shallow water communication have their own set of difficulties compared to Deep water communication. Certain elements, including as surface noise, temperature gradients, and the impact of multipath propagation due to reflections, have a greater impact in shallow water than in deep water. Therefore, a simple and comprehensive underwater acoustic communication model is designed here to reliably predict the propagation delay, transmission loss, multipath effect and bit error rate based on QPSK modulation for shallow underwater acoustic communication. Wenz model is used to determine ambient noise, and Thorpe's model is used to analyze the attenuation coefficient of the acoustic signal.

In this study, QPSK modulation with convolution coding is at the transmitter end, and a Viterbi decoder is at the receiver are implemented. An in-depth analysis of the Viterbi decoder is discussed by comparing various results obtained by varying the design parameters. The simulation results are used to select an improved Viterbi decoder, which is then implemented into an underwater wireless acoustic communication system. The foundation for multipath propagation modeling is the image method(i.e. Eight paths). Finally, the performance of the BER is simulated using a shallow water acoustic channel model.

CONTENTS

LIST OF TABLES

LIST OF FIGURES

CHAPTER 1

INTRODUCTION

1. INTRODUCTION

1.1 Overview

UNDER WATER ACOUSTIC (UWA) communications have been used in military applications for a long time. Acoustic waves are the preferred method for this particular circumstance because of their excellent water propagation properties, which permit underwater wireless communication.Radio waves are less effective for this because of their significant attenuation in water. Because optical waves scatter quickly, it will be necessary to use short-range, intense laser beams that are both narrow and powerful but inefficient over long distances for underwater data transmission. However, there are many ways in which the shallow-water acoustic channel is distinct from radio channels. The UWA channel has a finite amount of bandwidth that varies depending on frequency and range. Time-varying multipath has an impact on the acoustic signals and can lead to spreads and severe inter-symbol interference (ISI). The primary objective of the work is to simulate how environmental factors impact underwater transmission. The effects of spreading loss, scattering, and reflections must be taken into consideration in the mathematical formulation.

A shallow underwater communication system is a type of communication system that is used for transmitting information through water in relatively shallow areas such as coastal regions, lakes, and rivers. These systems are used for various applications, including underwater sensing, data collection, monitoring, and control of underwater equipment. Shallow water communication systems typically operate in the frequency range of a few kilohertz to several megahertz, depending on the range, data rate, and the type of information to be transmitted. Acoustic signals are commonly used for communication because sound waves can travel long distances in water, with minimal attenuation. The transmitter and receiver are typically the two major parts of these systems. The electrical signal is transformed by the transmitter into an acoustic signal, which is subsequently transferred through the water. The receiver then detects the signal and conversion back into an electrical signal for processing. One of the major challenges of shallow water communication is the presence of noise and interference, such as from other underwater equipment, marine life, and ocean currents. Therefore, signal processing techniques, such as filtering and signal detection algorithms, are employed to improve the quality of the received signal Applications for shallow water communication systems include environmental monitoring, underwater navigation, and underwater surveillance. They are also used in the industry for pipeline monitoring and in the fishing

industry for fish tracking. As underwater communication technology continues to advance, these systems will become increasingly important in a wide range of fields.

The following factors, in particular, effect underwater communications:

1.2 Channel Of Variations

Channel Of variation are due to changes

- Temperature
- Water Salinity
- Water PH
- water depth column or pressure
- Surface and bottom roughness

1.3 Multipath Propagation

The channel is commonly thought of as a waveguide, and the multipath travel of the signal happens as a result of reflections at the top and bottom of the channel.

1.4 Attenuation

Due to sound scattering by channel in homogeneities, a portion of the acoustic energy is absorbed into heat or lost.

1.5 Doppler Shift

The ray that hits off the water's surface is seen as a ray that is really being sent from a moving transmitter because of the shifting shape of the water's surface, which causes a Doppler shift in the signal that is received. The signal that was sent can be either compressed or extended at the receiver when the transmitter and receiver are moving closer to another. The Doppler effect is subsequently seen.

Higher speed of data and secure communication networks are hampered by channel fluctuations and propagation of multiple path. Additionally, at great distances, the useful bandwidth is often just a few kHz since of the increased absorption of higher frequencies.

The source employed may be a stream of bits, an ASCII text, an image file or maybe a video which are finally encoded as a stream of bits. Transmitter modulate bits into QPSK "Underwater Acoustic Channel (UAC)" receives the transmitter's output and its output in the form of symbols. The receiver block decodes the QPSK symbols to information bits, measures the sync time and offset phase, and analyses the sent signal.

This modulation technique is widely used in several applications like CDMA cellular service, wireless local loop, Iridium (a voice/data and satellite system) and DVB-S. In this project the idea of receiver design has been taken from these applications.

An in depth analysis of channel variations and multipath propagation are considered, in this report. Thus a consistent simulation environment is presented in underwater communication applications (decreasing the necessity of sea trials) that model the sound channel by incorporating multipath propagation, attenuation, surface and bottom reflection, spreading losses and scattering losses. With this analysis of underwater channel, a communication system is modelled, along with the combination of convolution encoder and Viterbi decoder for reliable underwater communication.

1.6 LITERATURE SURVEY

1. "Short-range underwater acoustic communications" by D. D. Lin et al. in IEEE Communications Magazine, 1997.

This paper provides an overview of the challenges and solutions for short-range underwater acoustic communications. The authors discuss the characteristics of the underwater acoustic channel, the effects of noise, multipath and interference, and different modulation and coding schemes for reliable communication.

2. "Short-range underwater acoustic communication using spread-spectrum techniques" by J. A. Catipon et al. in Journal of the Acoustical Society of America, 2005.

This paper describes the use of spread-spectrum techniques for short-range underwater acoustic communication. The authors demonstrate the effectiveness of direct-sequence spread-spectrum (DSSS) and frequency-hopping spread-spectrum (FHSS) modulation schemes in reducing the effects of interference and multipath propagation.

3. "Short-range underwater acoustic channel measurements and modeling" by F. Gao et al. in IEEE Journal of Oceanic Engineering, 2015.

This paper presents experimental measurements and modeling of the short-range underwater acoustic channel. The authors investigate the effects of environmental factors such as temperature, salinity, and sound speed on the channel characteristics, and propose a channel model for short-range underwater acoustic communication.

4. "Short-range underwater acoustic communications using multiple-input multiple-output (MIMO) techniques" by A. C. Boucouvalas et al. in IEEE Transactions on Communications, 2018.

This paper explores the use of multiple-input multiple-output (MIMO) techniques for short-range underwater acoustic communication. The authors propose a MIMO channel model for underwater communication and demonstrate the effectiveness of MIMO in improving the reliability and data rate.

5. "Short-range underwater acoustic positioning using acoustic signals of opportunity" by W. Hu et al. in Journal of Navigation, 2019.

This paper describes a novel approach for short-range underwater acoustic positioning using acoustic signals of opportunity, such as ambient noise and marine mammal vocalizations. The authors demonstrate the feasibility of this approach in a real-world experiment and show that it can achieve high positioning accuracy in shallow water environments. These papers provide a glimpse of the current research trends in short-range underwater acoustic communication, including channel modeling, modulation and coding techniques, MIMO, and novel positioning methods.

6 ."Design and performance analysis of QPSK modulation for shallow water acoustic communication systems" by M. A. Razzaque et al. (2016)

This paper presents the design and performance analysis of a QPSK modulation scheme for shallow water acoustic communication systems. The authors investigate the effects of shallow water channel characteristics on the performance of the QPSK modulation scheme.

7. "Experimental study of QPSK modulation in shallow water environment" by J. Zhao et al. (2017)

This paper presents an experimental study of QPSK modulation in a shallow water environment. The authors evaluate the performance of the QPSK modulation scheme in terms of bit error rate (BER) and signal-to-noise ratio (SNR).

8. "Performance analysis of QPSK modulation in shallow water channel using channel coding" by A. M. Hassan et al. (2018)

This paper investigates the performance of QPSK modulation in a shallow water channel using channel coding techniques. The authors evaluate the performance of different coding schemes in terms of BER and data rate.

9. "Adaptive QPSK modulation for underwater acoustic communication systems" by Y. Xie et al. (2019)

This paper presents an adaptive QPSK modulation scheme for underwater acoustic communication systems. The authors propose a method to dynamically adjust the modulation order of the QPSK scheme based on the channel conditions to improve the system performance.

10. "A comparative study of QPSK and OQPSK modulation schemes for shallow water acoustic communication" by S. Mandal et al. (2020)

This paper presents a comparative study of QPSK and OQPSK (Offset Quadrature Phase Shift Keying) modulation schemes for shallow water acoustic communication. The authors evaluate the performance of these two modulation schemes in terms of BER, SNR, and data rate.

Overall, these studies demonstrate the effectiveness of QPSK modulation in shallow underwater acoustic communication and highlight the importance of considering the specific

characteristics of the underwater channel when designing and evaluating communication systems.

CHAPTER 2

CONVOLUTION CODES CONSTRUCTION

2. CONVOLUTION CODES CONSTRUCTION

2.1 Overview

This chapter presents an effective and frequently used class code, called convolution codes , long term evolution systems, and 4G.These codes are also of high value because they are obtained through awareness rather than from reasoning or observation, so one can easily realize them in many ways. There is also a possible way to recover the most likely message which might be transmitted among the set of all available possibly transmitted messages.

Convolutional codes are slightly similar to the block codes. They involve the processing of input message bits in order to generate the parity bits. They, transmit only the generated parity bits hence deferring from the block codes, where the message bits are transmitted next to parity bits.

2.2 Code Construction of Convolution

The encoder makes use of a sliding window to calculate *'r'* i.e. the number of parity bits, by relating the subgroups of input message bits present in the window. This relation is an addition in F_2, (i.e., modulo 2 addition).In convolutional codes the windows overlap and slide by a step. The code's constraint length is defined as the window size, in bits. As the length increases the no of parity bit altered from the input message bit increases. The parity bits are bits that are transmitted through the channel, themore the constraint length's the greater is the flexibility to detect bit errors. The major back drop of using longer constraint lengths in convolution codes is that it effects the decoding complexity at the receiver. Hence, it is recommended to maintain an optimum constraint length to avoid decoding complexity and reduce, the processing time.

The parity bits *'r'* that are produced by the encoder defines the rate *'1/r'* of the convolution code. The chance of occurrence of bit errors is high if the value of '*r'* is high. Which conveys that the usage bandwidth of the channel is high as the redundancy increases in proportion with *'r'*.

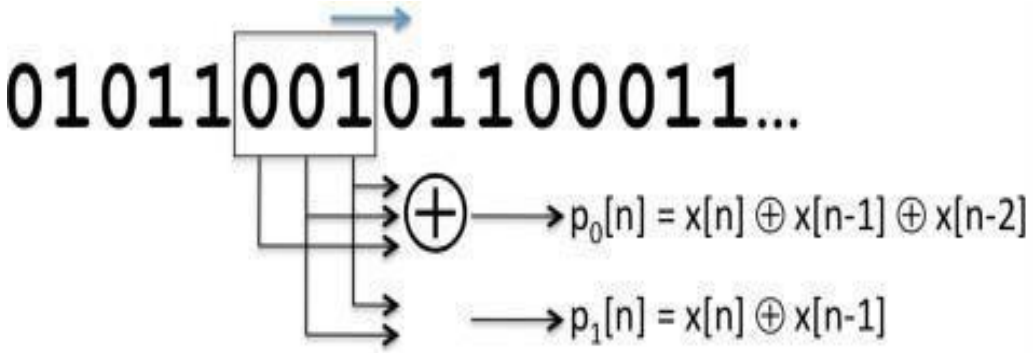

Figure 2.1. An example to represent comvolution code computation

It is recommended to pick the values of *'r'* and constraint length as minimum as possible. The notation *'K'* is used to refer to the constraint length. Furnished with this notation, the convolution code encoding process is described succinctly. As per the chosen functions to operate upon the subsets of 'K' bits, the convolution encoder works on all *'K'* bits in a single instant and produces '*r'* parity bits. An example of encoding with *'K'= 3* and *'1/r' = ½* convolution code polynomial .The *'r'* parity bits which are generated out by the encoder, are transmitted serially, then the window slides by one step i.e. one bit length to the right side, and then iterates the method. The particulars that are to be considered at the transmitter for encoding the message are listed below:

- Choosing of the parity generator function.
- How to denote the function conveniently?
- How to employ the encoder in an efficient manner?

It shows an example of one set of parity equations, which govern the way in which parity bits are produced from the sequence of message bits, *X*. The equations in the example, are as follows (all additions computed are in F_2)):

$$p_0[n] = x[n] + x[n-1] + x[n-2]$$
$$p_1[n] = x[n] + x[n-1] \quad (2.1)$$

A set of 1/3rd rate convolution encoder parity equations are given below:

$$p_0[n] = x[n] + x[n-1] + x[n-2]$$
$$p_1[n] = x[n] + x[n-1]$$
$$p_2[n] = x[n] + x[n-2] \quad (2.2)$$

Each parity equation stated above in general is produced by processing the *'x'* message bits with the selected generator polynomial *'g'*. From the first example above, it is noted that (1, 1, 1) and (1, 1, 0), are the ½ rate generator polynomial coefficients, where as in the second, (1, 1, 1), (1, 1, 0), and (1, 0, 1) are 1/3rd rate generator polynomials.

The *'K'*-element generator polynomials denoted by 'g_i' for a parity bit *'p_i'*. 'p_i' is given as follows:

$$[n] = (\sum_{j=0}^{k-1} g[j]x[n-j]) \bmod 2 \qquad (2.3)$$

The code is named as "convolution code" as it is evident from the equations that the parity bit generated is a result of convolution of *'g'* with *'x'*. The number of parity bits *'r'* generated is exactly same as the number of generator polynomials of the encoder.

For example, consider the generator polynomials defined by equations i.e. g_0 and g_1.

$$g_0 = [1\ 1\ 1]$$
$$g_1 = [1\ 1\ 0] \qquad (2.4)$$

TABLE 2.1. Some of the generator polynomials for 1 / 2 rate convolutional codes

Constraint length	G_1	G_2
3	1 0 1	1 11
4	1 0 1 1	1 1 1 1
5	1 0 1 1 1	11 0 0 1
6	1 0 1 1 1 1	1 11 1 0 1
7	1 0 0 1 1 1 1	1 1 0 1 1 0 1
8	1 0 1 1 0 1 1 1	1 1 1 1 1 1 0 1
9	1 0 0 1 0 1 1 11	1 1 1 1 0 1 1 0 1
10	1 0 0 0 1 1 11 1 1	1 1 0 1 1 0 1 1 0 1

If the message's order is [1 0 1 1...], then X = The parity bits from Equation 2.1 thus form (as usual, x [n] = 0 n 0)

$$p_0[0] = (1 + 0 + 0) = 1$$
$$p_1[0] = (1 + 0) = 1$$
$$p_0[1] = (0 + 1 + 0) = 1$$
$$p_1[1] = (0 + 1) = 1$$
$$p_0[2] = (1 + 0 + 1) = 0$$
$$p_1[2] = (1 + 0) = 1$$
$$p_0[3] = (1 + 1 + 0) = 0$$
$$p_1[3] = (1 + 1) = 0 \qquad (2.5)$$

[1 1 1 1 0 0 0 0 . . .] are the parity bits that are transmitted by the transmitter. Out of the mostly available generator polynomials finding out the polynomials which are efficient is still out of reach. Some of the used polynomials

2.3 Convolutional Encoder

This section deals with the description of a convolution encoder, which improves the understanding capability of the user. It also briefly explains how to encode and decode convolution codes .First method is particulars of block diagram , The mechanism is formulated with the help of shift registers that are joined together. The second method deals with respect to state , which corresponds with well-illustrated state transition among the available states. This method turns out to be utterly beneficial in finding out the way to decode set parity bit, to find out the message bits transmitted.

Block Diagram

It shows the block diagram of a similar encoder. The x [n − 1] values (two in this situation) are assigned to as the states of this encoder. The block schematic is viewed as a "black box" that lets parity bits in and message bits leave. The black-box's input receives the supplied message bits, x [n], from the left. From the concept of the incoming bits and the current state of the encoder, which is identified by the 'k1' prior bits, the black box produces the parity bits.

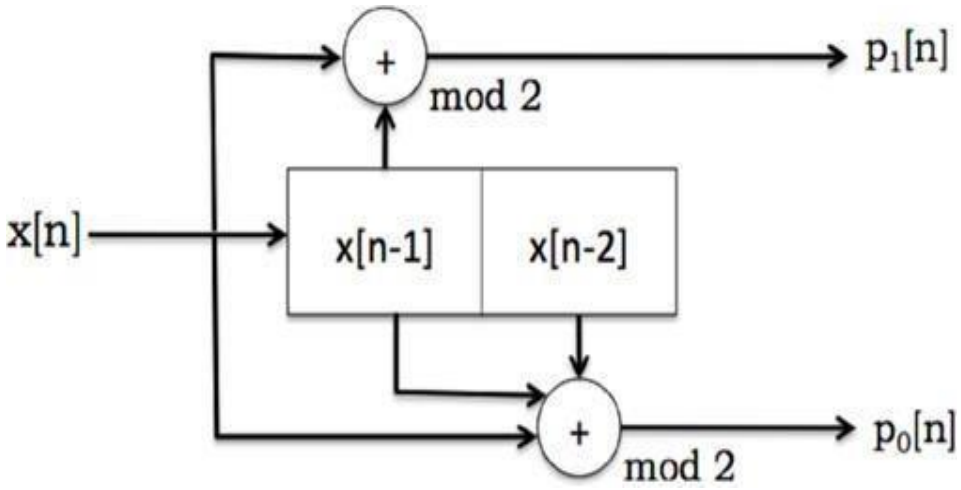

Figure 2.2. Shift register representation of a convolution encoder.

State transition takes place i.e. by one state when '*r*' parity bits are generated by the encoder, the state shifts from, x [n] to x [n−1], x [n−1] takes the place of x [n−2]… x [n − K + 1] , with x [n − K + 1] being discarded at the end.

State Machine

Another method of representing convolutional codes is a state machine. The state machine is same for all the convolution codes whose constraint length remains constant as *'K'*.

Only the p_i label the change depending on number of a generator polynomial along with their coefficient values. Each state is defined as x [n − 1] x [n − 2] ..... x [n − K + 1]. Each arc is defined as x [n] /p_0p_1, x [n-1] /p_0p_1, … x [n- K+1] /p_0p_1 and so on. In the example illustrated, input message [1 0 1 1 0 0] is considered as an example, and the encoded sequence [11 11 01 00 01 10] is transmitted.

It is exquisite to summarise the operation of the convolution encoder at the transmitter by representing convolution codes as a state machine. It also provides information on how to decode the stream of bits that was received at the receiver.

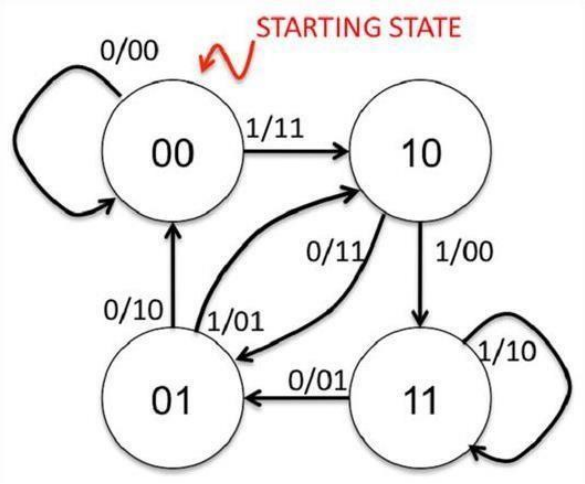

Figure 2.3. State machine representation of convolutional coding.

The encoder initiates at the initial state (shown as "STARTING STATE" and then process each incoming message separately. According to the incoming bit value, a state occurs for each incoming message bit, producing the parity bits in the process.

The receiver, as usual, is not aware of the state transitions at the encoder. It only has the knowledge of the sequence of parity bits received at the decoder input, with some probable error bit.

2.4 Difficulty in Decoding

As stated above, the decoder should be able to find out the "best possible" sequence of the transitioned states at the encoder. There are many ways in finding the *"best"*, but the one which is distinctly interesting is the *"most likely"* sequence of states which can be traversed by the encoder. The decoder which is capable of determining the *"most likely"* sequence is the "maximum likelihood" decoder. Determining the nearest code word to a received code word is not so easy, to do for convolution codes.

It illustrates a convolution of code k = 3 and 1/2 rate .The code word received atthe decoder is [11 10 11 00 01 10], then there is a chance of occurrence of errors, because there is no valid encoder sequence that matches the received sequence. The hamming distance i.e. *'d'* is listed in the last column of which gives the most likely distance to all the

probable encoded sequences from the present sequence, with the least distance highlighted. To decide the most-likely message, the decoder has to check for the sequence with lowest value of hamming distance, from the received sequence at the input of the decoder.

It is quite challenging to examine the list of possible message sequences that may have been broadcast and compare hamming distances due to the 2N potential code words for a given sequence of N bits. Code words for an N-bit transmission sequence. Therefore, a strong concept is required at the receiver in order for the decoder to swiftly traverse through this enormous field of possible outcomes and choose the "most-likely" message with the shortest hamming distance. In the next chapter, a practical and often used approach to resolving this issue is covered. This technique makes use of an original framework known as the "trellis," which is covered in the next section.

CHAPTER 3

VITERBI DECODING

3.VITERBI DECODING

2.5 Overview

This chapter portrays an exquisite and productive technique to unravel convolution codes ,Those development , encoding is depicted in the before chapter . This unraveling strategy dodges expressly, specifying the 2^N code words groupings of N bit parity. Andrew Viterbi developed this system, which carries his name.

2.6 Problem in Decoding

Voltage samples which are analogous to the generated parity bits are present in sequence at the decoder input, that are transmitted by the encoder. At the receiver a suitable algorithm picks up the samples and propagates these samples for the next stage of processing.

Thus, a sequence of received samples are available which corresponds to the stream of parity bits generated by the convolutional coding of message bits at the transmitter. These samples are directly picked up for decoding or are digitized to “1” or “0” by comparing the sample values with the threshold.

If the digitized samples are utilized in decoding these convolution codes the decoding process called “hard decoding”. But if the actual voltage samples are utilized in decoding, then the process is called as “Soft decoding”.

Hard decoding or soft decoding can be performed by the Viterbi decoder. Possibly, that hard decision decoding settles on an early choice in case a bit be ‘0 or 1’, as it discards a little amount of information in the process of digitizing. It introduces few bit errors in the decoded bit sequence as it is not sensitive to the voltage values which are closer to the threshold value, hence making a wrong decision.

However, by adding more faults during the initial stages of digitization, it still creates most-likely message sequence that delivered when received bit is supplied at the decoder. The chance of bit mistake drops relatively slightly as compared to soft choice decoding. However, it is fundamentally easier to comprehend the "hard decoding" method.

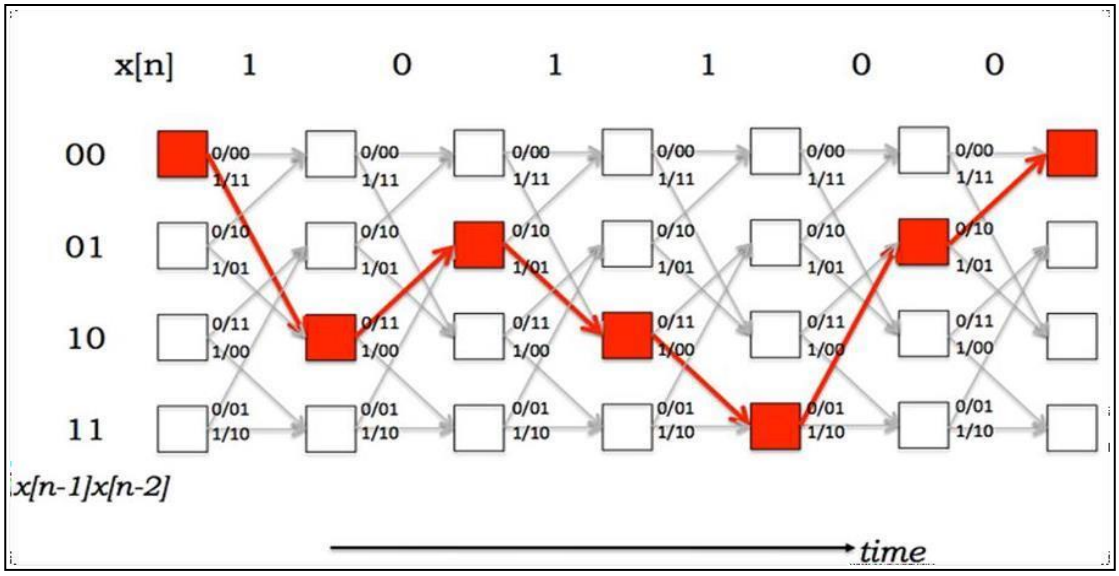

Figure 3.1. Trellis structure implementation of a state.

We discussed in the before chapter the trellis structure provide a method to understand the decoding procedure for convolutional codes . For a sequence of digitized bits at the decoder it is assumed that the complete trellis structure is available for a given code. A path always exists traversing the sates of the trellis structure for high SNR value i.e. when there are no bit errors which possibly match with the received bit sequence. This path relates to the parity bits transmitted by the encoder. From the available path finding out the original message sequence is easy as the direction of the next state with relative to the present sate in the trellis, reflects the message bit transmitted. When the next state is above the present sate or at the same level, it reflects that a "0" bit is transmitted and if the next state is below the present state, it reflects that a "1" bit is transmitted.

It's interesting to know how the trellis helps in decoding when bit errors occur. It explained early finds the most likely encoded messages of sequences is fascinating, this helps in minimizing the BER. Finally, the path which results out with the least sum of errors is the desired path. Hence, from this desired path the message is decoded.

2.7 The Viterbi Decoder

Two metrics are handy in The Viterbi decoding algorithm [8]; known as the "Branch Metric (BM)" and the "Path Metric (PM)". The distance between the transmitted code-word and the received code-word is defined as the Branch Metric and it is marked for each arrow

in the trellis. As the digitized parity bit sequence is provided in “hard decision decoding” the hamming distance calculated is the branch metric.

Considering an example illustrated in 3.2, where the received set of parity bit are 00. The first stage of trellis it is observed that the branch metrics of two transitions are 0, implying the corresponding hamming distance of 0 for the state transition .The value of branch metric is shown on the arrow of the trellis structure for that particular state transition. The remaining non-zero branch metrics implies the presence of bit errors during the transmission.

The metric usually associated with a state in the trellis structure is the path metric. It implies the sum of all the hamming distance over the most likely path, starting from the initial state in the trellis to the current state. “Most likely path” implies the path with the smallest Hamming distance of all possible paths between the two states. This most likely path with the smallest Hamming distance minimizes number of bit errors when the BER is low.

The key perceptiveness in the Viterbi decoding algorithm is that at the receiver it is able to calculate the “path metric” for a state, time pair cumulatively making use of the path metrics computed from the branch metrics of the previous states and the present state.

2.8 Computation Of Path Metric

Let's say that the receiver has listed the path metric PM [s, i] for each state "s" at a time step "i" there are 2K states, and "K" is the length of the codes' constraint.The value of PM [s, i] in “hard decision decoding” is the total number of bit errors detected, as a result of comparing the most likely transmitted message with the received parity bits, considering all the probable message sequences that could have been transmitted by the transmitter until time step *‘i’* (originating from state “00”, which is always taken as initial state, by convention).

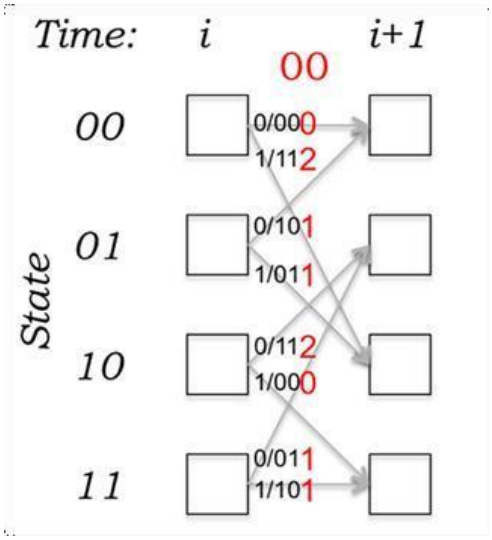

Figure 3.2. The complex decision decoding branch metric

The most likely state from all the possible states at the time step instant 'i' is the one with the minimum path metric. All the states with the minimum path metric at that instant are in good position to be a part of the most likely path.

Now, how can the path metric be determined at time step i+ 1, PM [*s*, *i*+ 1], for each state '*s'*? To find out the solution of this question, initially notice the state of the transmitter '*s'* at the time step i+ 1, then *"it must have been in only one of the two states possible at time step i"*. These two states are termed as the *predecessor states*, and are labelled as "*α"* and "*β"*, these states are always the same for the given state. These predecessor states changes with respect to constraint length only.

It must be noted that any of the message sequence that the transmitter transmits in state 's' at the time i+1 must have been in state *α* or state *β* at time 'i' at the transmitter. For example, as in Figure 3.2, in order to reach the state "01" at time 'i+1', one of the two properties given below must be valid:

- The transmitter might be in state 10 at time instant '*i'* and the i^{th} message bit was a "0".If this is the case, the parity bits transmitted by the transmitter are "11", as the received bits are 00 the number of bit errors is two. Hence, the new states path metric PM [01, i+1] is equivalent to PM [10, *i*] +2,

because the new state is “01” and the corresponding path metric is larger by two because of the presence of two errors.

- The transmitter being in state 11 at instant "i" and the I th message bit being "0" are the remaining possibilities. If this is the case, it can be deduced that the transmitter sent the parity bits 01 and received 00, resulting in a bit error. The new state's path metric, PM [01, i + 1," is the same as PM [11, i] + 1. In light of the preceding instinct, it can be deduced that

$$PM[s, i+1] = \min(PM[\alpha, i] + BM[\alpha \rightarrow s], PM[\beta, i] + BM[\beta \rightarrow s]) \quad (3.1)$$

α and β being the two previous states. It is important to remember in the decoding process that which arrow corresponds to the minimum, because it is needed to traverse back only through this path from the final state to the initial one keeping a track of the arrows used, and then finally reverse the order of the bits to produce the most likely message.

2.9 Most Likely Path

Look into how the decoder discovers the maximum-likelihood path. Initially, state “00” has a metric of ‘0’ and the remaining $2^{k-1}-1$ states have a metric of ∞.The main loop of the algorithm consists of two main steps:

1. Branch metric calculation the for the next set of parity bits.
2. Path metric computation for the next column.

Add-compare-select procedure is implemented for the computation of path metric:

1. To refresh the way metric add branch got, to way metric of old state.
2. Compare the sums of the path metric for each of the paths that arrive at new state (there two of these paths compare at new state because only two incoming arrows from column before that).

3.For breaking the ties arbitrarily, the path which has the smallest path metric is to beselected. This path is the most likely path which corresponds to the one with few errors.

This explains how the Viterbi decoder algorithm performs the decoding process step by step. This example illustrations a received bit sequence of [11 10 11 00 01 10] and how the “Viterbi Algorithm” processes it. The second picture shows the states having the same path metric.

Any state among the four states at this stage and paths leads up these states are the likely transmit bit sequences with having the hamming distance of 2. The survivor path defines as the discard because cant be most likes at any means.

This keeps going with the illustration until the transmitted message's most likely content is determined by decoding all of the parity bits that were received. Use the final state with the smallest path metric as a starting point, work backwards, reverse the bits order, and you'll get this message. So that the backward pass can be executed correctly

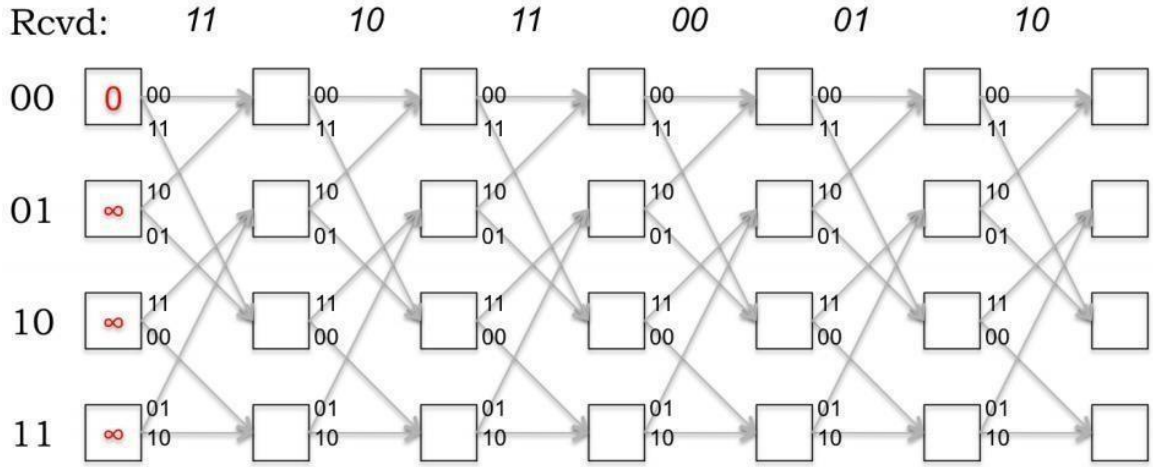

Figure 3.3. The Viterbi decoder mechanism initial stage.

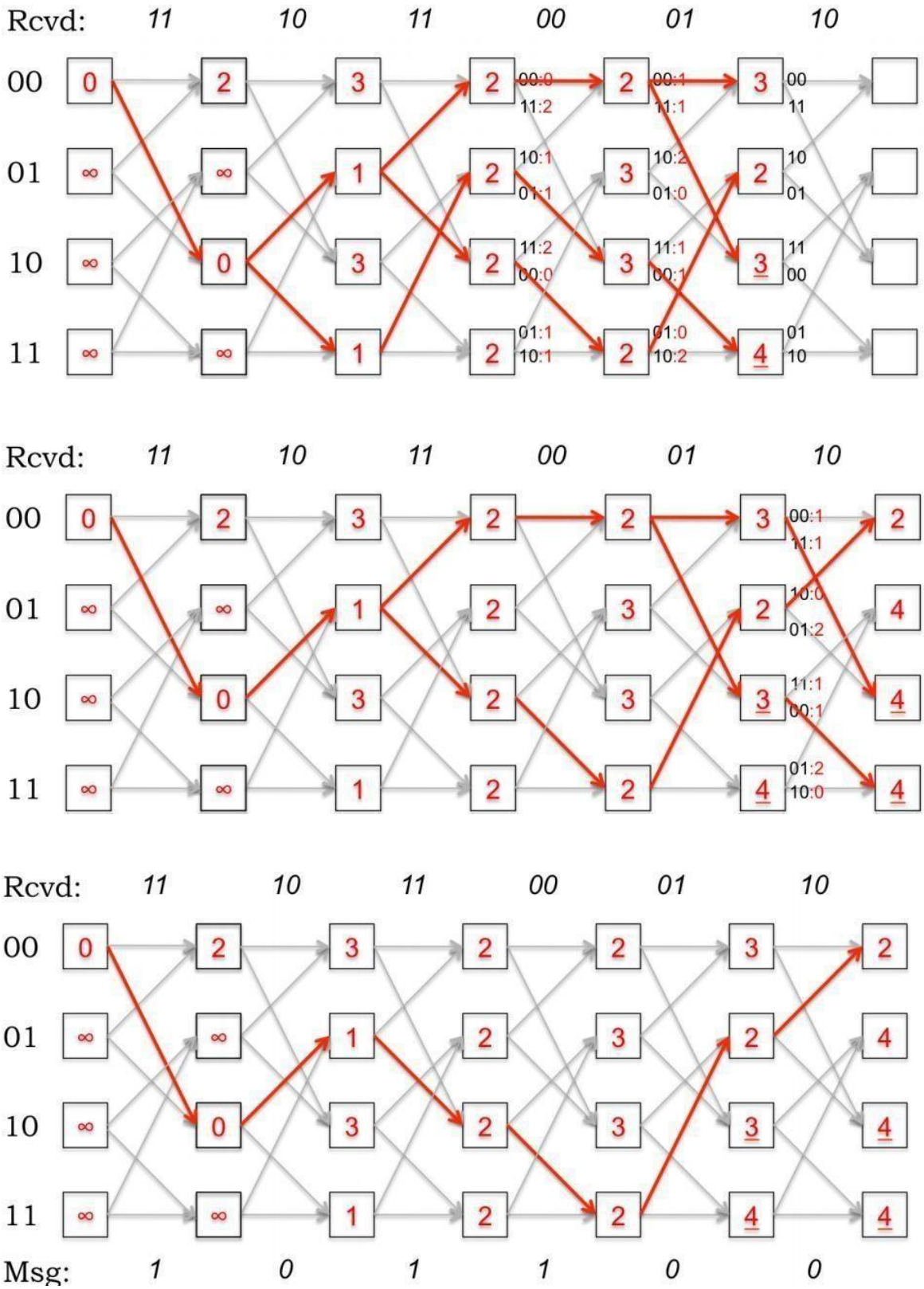

Figure 3.4. The Viterbi decoder mechanism in detail , The decoded message is shown at the end.

CHAPTER 4

UNDERWATER CHANNEL CHARACTERISTICS

4. UNDERWATER CHANNEL CHARACTERISTICS

- Speed of sound
- Propagation loss
- Reflection of the sea surface
- Reflection from bottom of sea
- Acoustic signal level
- Signal attenuation
- Spreading loss
- Absorption loss
- Path loss

4.1 Overview

Underwater channels are channels of water bodies such as rivers, lakes, and oceans that are characterized by specific features. Some of the characteristic features of underwater channels include:

Depth: Underwater channels are typically deeper than their surrounding areas. This depth can vary greatly depending on the location, ranging from a few meters to several kilometers.

Width: The width of an underwater channel can vary depending on the type of water body it is found in. For example, rivers typically have narrower channels than oceans.

Currents: Underwater channels are often characterized by strong currents, which can be caused by a variety of factors such as tides, wind, or water temperature differences.

Turbulence: Turbulent water flow is common in underwater channels, and can be caused by a variety of factors such as changes in depth or direction of the channel, or the presence of underwater obstacles.

Sediment transport: Underwater channels are often responsible for the transport of sediment, such as sand or gravel, from one area to another.

Biological activity: Underwater channels can be home to a variety of marine life, including fish, plants, and other organisms.

Acoustic properties: The underwater environment can affect the propagation of sound waves, with underwater channels often exhibiting different acoustic properties than surrounding areas. This can have implications for underwater communication and sensing systems.

Overall, the characteristics of underwater channels can vary greatly depending on the location and environmental conditions, but they are an important and complex feature of aquatic systems.

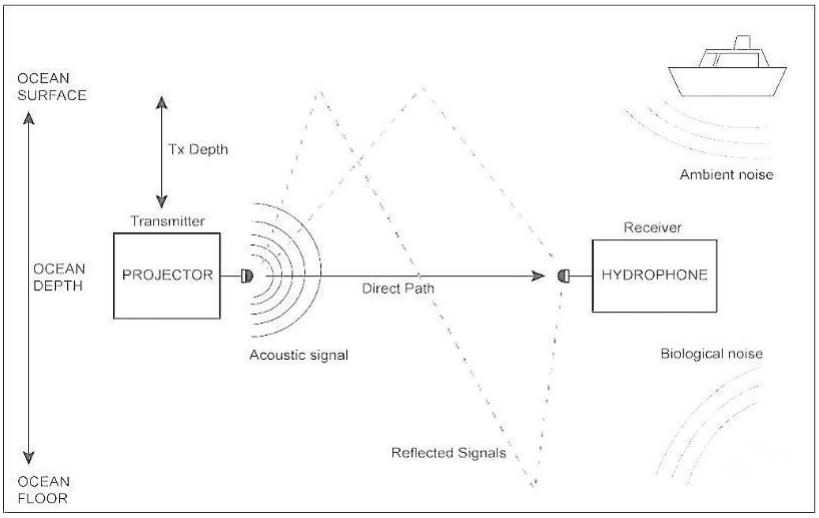

Figure 4.1. Underwater acoustic communication environment

Speed of sound:

The Mackenzie equation which calculates the speed of sound in water is given as

$$v = 1448.96 + 4.591C - 5.304 \times 10^{-2}C^2 + 2.374 \times 10^{-4}C^3 + 1.340 (S-35) + 1.630 \times 10^{-2}D + 1.675 \times 10^{-7}D^2 - 1.025 \times 10^{-2} C(S-35) - 7.139 \times 10^{-13} CD^3 \quad (4.1)$$

v = sound speed in m/s

C = temperature in degree Celsius

S = salinity in parts per million (ppt)

D = depth in meters

Propagation loss:

The loss of acoustic energy as an underwater sound wave moves away from its source (due to attenuation and/or spreading).

$$PL = 20\ 1og\ R + \alpha\ R\ (m^{-1}) \quad (4.2)$$

R = Distance

α = Absorption coefficient

Acoustic Signal Level:

The projector source level, $SL_{tprojector}$, is generally defined in terms of the sound pressure level at a reference distance of 1m from its acoustic centre. The source intensity at this reference range is I = p_{tx}/Area (W/m^2) and measured in dB 're 1 μPa' but strictly meaning 're the intensity due to a pressure of 1 μPa'. The amount of energy per unit time is power therefore, the intensity is the amount of power transmitted through a unit area in a specified direction I=power/Area (W/m^2) Omni directional area is a sphere ($4\pi r^2$12.6m^2).

$$\mathbf{SL_{tprojector} = 10\ log\ \left(^{tx}/_{\frac{I_{ref}}{12.6}}\right)\ dB} \quad (4.3)$$

Where $p\ tx$ =total acoustic power consumed

I_{ref} = reference wave intensity

we know that , pressure a $\frac{1}{r}$, Intensity a $\frac{1}{r2}$

P^2 a $\frac{1}{r2}$ → P^2 a Intensity(I)

$I = \left(\frac{P^2}{p*c}\right)$

$I_{ref} = \frac{(Paref)2}{p*c}\ (wm^{-2})$

where, $paref$ = 1 μPa (Reference Pressure Level)

p = density medium

c = speed sound

[avg sea water : p= 1025 Kg/m^3 , c = 1500 m/s]

$$\mathbf{SL_{projector}(P) = 170.8 + 10log_{Ptx}\ dB} \quad (4.4)$$

$$\mathbf{DI_{tx} = 10log\left(\frac{Idir}{Iomni}\right)} \quad (4.5)$$

$Iomni$ = Intensity if spread spherically

$Idir$ = Intensity along axis of beam pattern

$$\mathbf{SL_{projector}\ (P, \eta, DI) = 170.8 + 10logP_{tx} + 10log\eta_{tx} + DI_{tx}dB} \quad (4.6)$$

Signal attenuation:

The acoustic signal underwater experiences attenuation due to spreading and absorption. Path loss is the measure of the loss signal intensity from projector to hydrophone.

Spreading loss:

Spreading loss is due to the expanding area that the sound signal encompasses as it geometrically spreads outward from the source.

$$\mathbf{PL_{spreading}(r) = k * 10log(r)\ dB} \quad (4.7)$$

r = range in meters

k = spreading factor

When the medium in which signal transmission occurs is unbounded, the spreading is spherical and the spreading factor k=2.

whereas in bounded spreading, considered as cylindrical k=1.

Absorption loss:

The energy loss expressed in the absorption loss takes the form :heat generated through ionic relaxation and viscous contact as a result of an auditory signal's wave. $PL_{absorption}(r, f) = 10\log(f) * r$ dB.(4.8)

r= range in km and absorption factor

Over the last fifty years, changes in absorption losses have given rise to a number of empirical equations thataccount for frequency, salinity, temperature, PH, depth, and sound speed.

Thorp's equation has a common version that applies to frequencies between 100 Hz and 1 MHz and is based uponseawater at 4 °C, PH 8, 35% ppt salinity, and 0 m depth.

$$\alpha(f) = \frac{0.11f^2}{1+f^2} + \frac{44f^2}{4100+f^2} + 2.75 \times 10^{-4} f^2 + 0.0033 \text{ dB/Km} \quad (4.9)$$

The effects of boric acid relaxation on absorption were discovered by Fisher and Simmon in the late 1970s, and they also provided a more precise form of the absorption coefficient alpha in db/km, which varies with frequency, pressure (depth), and temperature (valid for 100Hz to 1MHz with salinity 35% ppt, and acidity 8PH).$\alpha(f, d, t) = \frac{A1f1f^2}{f1^2+f^2} + \frac{A2p2f2f^2}{f2^2+f^2} + A_3P_3f^2$ dB/Km (4.10)

Path Loss:

Total path loss is the combined contribution of both the spreading and absorption losses. Uric (1967) established that this formula of spreading plus absorption yields a reasonable agreement with long range observations.

$$\mathbf{PathLoss(r, f, d, t) = k * 10log(r) + \alpha(f, d, t) * r * 10^3} \quad (4.11)$$

For very short range communication (below 50 m), the contribution of the absorption term is less significant than the spreading term. As range increases and the absorption term begins to dominate, any variations in α also becomes more significant. For data communication, the changes in the attenuation due to signal frequency are particularly important as the use of higher frequencies will potentially provide higher data rates.

Noise Modeling:

Under water channel noise is mathematically modelled, by considering the combination of the turbulence, shipping, wind and thermal noise. Most of the ambient noise sources can be described Gaussian statistics and a continuous Power Spectral Density (PSD). The following empirical formulae give the PSD of the four noise components in dB are µPa per Hz as a function of frequency in kHz is as given below:

$$10\log N_{turb}(f) = 17 - 30\log(f) \quad (4.12)$$

$$10\log N_{ship}(f) = 40 + 20(s - 0.5) + 26\log(f) - 60\log(f + 0.03) \quad (4.13)$$

$$10\log N_{wind}(f) = 50 + 7.5w\,1/2 + 20\log(f) - 40\log(f + 0.4) \quad (4.14)$$

$$10\log N_{th}(f) = -15 + 20\log(f) \quad (4.15)$$

Where N_{turb}, N_{ship}, N_{wind} , N_{th} stand for turbulence, shipping, wind and thermal noise respectively.

Travel Times

The time taken for each ray to reach the receiver is its travel time. From the above discussion it is evident that, all the other paths have more travel time compared to the direct path. Travel times for all the rays are easily computed if the length's or distances of all rays and the velocity of each ray are provided, the distances of all rays are known and the velocity of each ray is the speed of sound, '*c'*. Hence, the travel times of the rays is given as:

$$T_i = {}^{L_i}/_{C} \quad i = 0,1,2,\dots n \tag{4.16}$$

It show the delay of rays in two dimensional and three dimensional views. It is clearly observed that the delay of sinc pulse varies from ray 1 to ray 8. Here, sinc pulse is just considered as an example to show the concept of delay.

Grazing angle

Grazing angle is the angle with which each ray grazes the boundaries. This grazing angle is quite important because it influences both the bottom and surface reflection coefficients. With the help of mathematics, the grazing angle for the four paths or for all the rays, is given by the following equations:

$$\varphi_{m1} = \tan^{-1}\left(\frac{(2Dm)-z_s+z}{r}\right) \tag{4.17}$$

$$\varphi_{m2} = \tan^{-1}\left(\frac{(2Dm)+z_s+z}{r}\right) \tag{4.18}$$

$$\varphi_{m3} = \tan^{-1}\left(\frac{(2D(m+1))-z_s-z}{r}\right) \tag{4.19}$$

$$\varphi_{m4} = \tan^{-1}\left(\frac{(2D(m+1))+z_s-z}{r}\right) \tag{4.20}$$

4.2 Underwater multipath characteristics:

Multi-path propagation caused by boundary reflections at the sea-floor or sea-surface. Multi-path propagation caused by reflection from objects suspended in the water, marine animals or plants or bubbles in the path of the transmitted signal. Surface scattering caused by sea-surface (waves) or sea-floor roughness or surface absorption, particularly on the sea bottom depending on material. Volume scattering caused by refractive off objects suspended in the signal path.

4.3 Modeling of the multipath effect:

In shallow underwater acoustic communication systems, channel modelling is an essential aspect of designing and optimizing the performance of the system. The underwater acoustic channel is highly dynamic and can vary significantly over time and distance, due to various factors such as water temperature, salinity, pressure, and the presence of marine life and other environmental factors.

There are several approaches to modelling the underwater acoustic channel. One common approach is to use statistical models, such as the Rayleigh or Ricans distribution, to represent the channel impulse response. These models assume that the channel response is random and can be characterized by its statistical properties.

Another approach is to use physics-based models, which rely on the principles of wave propagation and acoustic scattering in water. These models can be more accurate than statistical models but are also more complex and computationally intensive.

One important consideration in channel modelling is the impact of multipath propagation, which occurs when sound waves are reflected, refracted, and diffracted by various objects in the water, such as the seafloor, the water surface, and underwater structures. Multipath propagation can result in signal distortion, interference, and fading, which can degrade the system's performance. Therefore, it is important to model the multipath propagation accurately and account for its effects in the system design.

In addition to multipath propagation, other factors such as ambient noise, Doppler shift, and channel attenuation also need to be considered in channel modelling. Signal processing techniques such as equalization and error correction coding can be used to mitigate the effects of these factors.

Overall, accurate channel modelling is essential for designing and optimizing the performance of shallow underwater acoustic communication systems, and researchers continue to develop new and improved modelling techniques to address the unique challenges of this type of communication system.

In the process simulation, the number of channel paths varies as a multiple of four. In the considered model, for the wave propagation from the transmitter to the receiver, we use four

Eigen paths. The transmitted wave either follows one of the four Eigen paths or a multiple of them.

In the case of multiple reflections, after several reflections, the wave reaches the receiver in one of the four ways.

$$P(r,z,\omega)=A(\omega)\sum_{m=0}^{\infty}\left\{\begin{array}{l}\hat{R}_1{}^{m}(\varphi_{m_1},\omega)\hat{R}_2{}^{m}(\varphi_{m_1},\omega)\dfrac{e^{-jkL_{m_1}}}{L_{m_1}}\\ +\hat{R}_1{}^{m+1}(\varphi_{m_2},\omega)\hat{R}_2{}^{m}(\varphi_{m_2},\omega)\dfrac{e^{-jkL_{m_2}}}{L_{m_2}}\\ +\hat{R}_1{}^{m}(\varphi_{m_3},\omega)\hat{R}_2{}^{m+1}(\varphi_{m_3},\omega)\dfrac{e^{-jkL_{m_3}}}{L_{m_3}}\\ +\hat{R}_1{}^{m+1}(\varphi_{m_4},\omega)\hat{R}_2{}^{m+1}(\varphi_{m_4},\omega)\dfrac{e^{-jkL_{m_4}}}{L_{m_4}}\end{array}\right\} \quad (4.21)$$

In this criterion, A is the amplitude of the sound wave; R1 and R2 are the reflection coefficients of the surface and bottom, respectively; ,…, are the reflection angles of the four Eigen rays; K is the wave number; and Lm1 , Lm2 , Lm3 , Lm4 are the lengths of the displacement vectors of the Eigen paths RSRBR, RBR, RSR, DP in the $(m+1)^{th}$ stage of the production cycle of virtual resources, respectively. Considering the location of the generated image in the m^{th} stage.

$L_{m1} = \sqrt{r2 + (2Dm - zs + z)2}$

$L_{m2} = \sqrt{r2 + (2Dm + zs + z)2}$

$L_{m3} = \sqrt{r2 + (2(m+1) - zs - z)2}$

$L_{m4} = \sqrt{r2 + (2(m+1) + zs - z)2}$…… respectively we find for 8 paths. (4.22)

Above each of the reflection coefficients of the surface or bottom is calculated based on the introduced pattern of that section. considering m=1 (i.e. eight paths), so the fifth path on, due to strong attenuation of the transmitted wave, there was no signal reception.

CHAPTER 5

OBSERVATIONS AND RESULTS

5.OBSERVATIONS AND RESULTS

5.1 Overview

Results from the simulation are presented in this chapter along with some intriguing findings. Learn about underwater acoustic channels first, and then discuss the system's communication component. The multipath propagation of an underwater channel is the primary determinant of effect. Since achieving high data rates with good transmitter and receiver geometry, or low BER, is the ultimate aim. The physical placement of a transmitter and receiver in an underwater acoustic channel with a depth "D" and an infinite length is referred to as geometry in this context. The multipath signal takes significantly longer than the straight path to reach the receiver at closer ranges.

5.2 Underwater Acoustic Channel

For various environment scenario described by the source location (z,z_s) receiver locations (r,rs),sound velocity, water depth, salinity, water temperature, pH values Figure 6.1 explains the impact of distances on time delays of multipath propagation for the following values considering the zero effect of losses ignoring wind speed and bottom type.

Environmental Scenario 1 :

TABLE 5.1. Various parameters for simulation of delay's for UAC.

Parameters	Design Values
Source Locations	$(z,z_s)=(0,20)$m
Receiver Locations	$(r,r_s)=(100,70)$m
Water depth	80m
Sound velocity	1500 m/s
Salinity	35ppt
Water Temperature	14(degree Celsius)

Bottom type	bt = 1 (core sand) With mean grain size is 0.5 and roughness Is 1.85cm
Wind speed	Vw=8
pH	8

In comparison to a desirable range of 1000 m, there is a significant difference in the relative travel times for very short distances of 10 m. The shorter distances cause the grazing angles to be very high. The relative travel times and grazing angles for rays hitting the surface or bottom, surface-bottom-surface or bottom-surface-bottom, etc., are another similar observation. This is caused by the fact that the transmitter and receiver are situated at precisely half the depth of the channel.

Only the time delay concept is highlighted here. As the lengths or distances of each ray are taken into account when calculating the grazing angle, we will now primarily use those angles to explain how the system behaves.the effects of transmission loss (including time delays) on multipath propagation over a range of horizontal and vertical transmitter and receiver depths. Changing the vertical depths involves moving the receiver closer to the surface or closer to the bottom in order to observe the exact behaviour of the bottom and surface reflection coefficients.

When they are 10 to 200 metres apart, multi-path propagation has less of an impact, which greatly reduces the complexity of the receiver design. In practical applications, a distance greater than 500 metres is typically desired between the transmitter and receiver. Therefore, all simulation results are presented with a 1000 m distance between the transmitter and receiver in mind. However, some simulation results are presented when the receiver and transmitter are closer together. Changes in the vertical depths of the transmitter and receiver are another factor taken into account in the simulation results that follow. These are only

displayed to demonstrate the effect of transmitter and receiver distances.

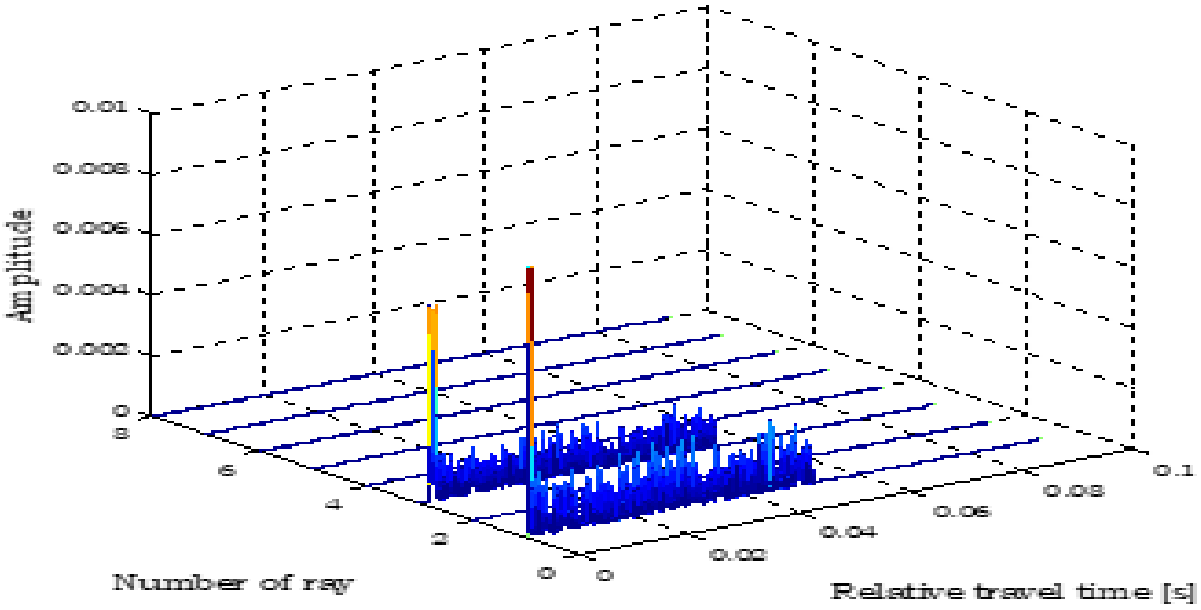

Figure 5.1. (Z,Z_S) = (0,20) and ((R,R_S) = (100,70)

TABLE 5.2. Various parameters for simulation of delay's for UAC.

Parameters	Design Values
Source Locations	(z,z_s)=(0,70)m
Receiver Locations	(r,r_s)=(100,20)m
Water depth	80m
Sound velocity	1500 m/s
Salinity	35ppt
Water Temperature	14(degree Celsius)
Bottom type	bt = 1 (core sand) With mean grain size is 0.5 and roughness Is 1.85cm
Wind speed	Vw=8
PH	8

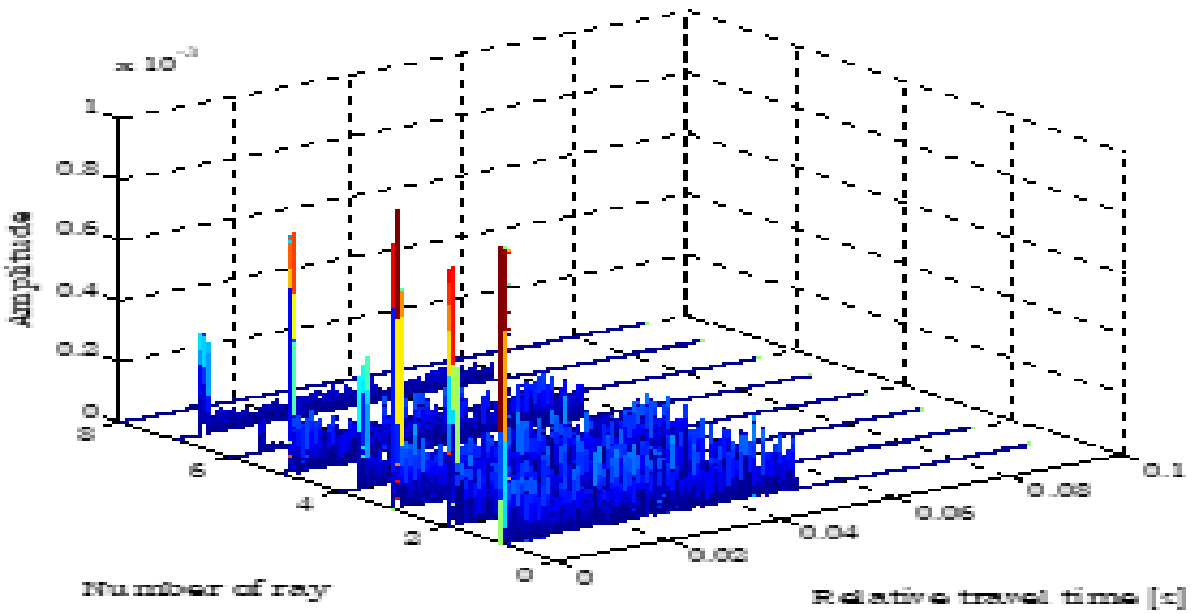

Figure 5.2. (Z,Z_S) = (0,70) and ((R,R_S) = (100,20)

Simulation results showing relative travel times for various transmitter and receiver locationsof a sine pulse including the transmission loss phenomenon for the scenarios .

Environmental Scenario 2 :

TABLE 5.3. Various parameters for simulation of delay's for UAC.

Parameters	Design Values
Source Locations	(z,z_s)=(0,20)m
Receiver Locations	(r,r_s)=(1000,70)m
Water depth	80m
Sound velocity	1500 m/s
Salinity	35ppt
Water Temperature	14(degree Celsius)

Bottom type	bt = 1 (core sand) With mean grain size is 0.5 and roughness Is 1.85cm
Wind speed	Vw=8
pH	8

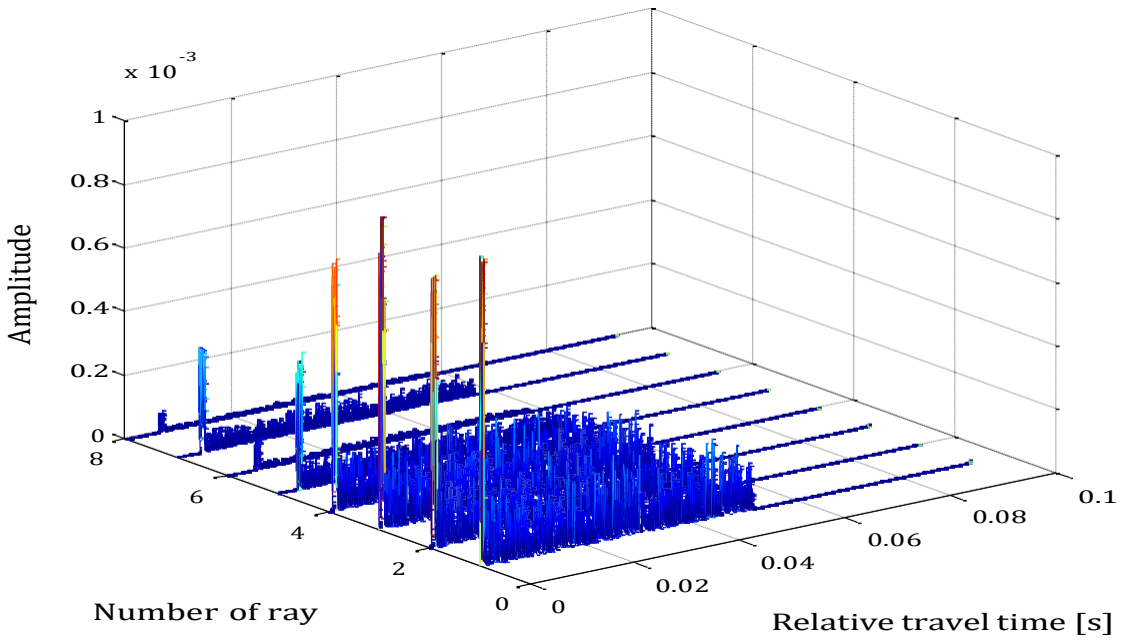

Figure 5.3. $(Z,Z_S) = (0,20)$ and $(R,R_S) = (1000,70)$

TABLE 5.4. Various parameters for simulation of delay's for UAC.

Parameters	Design Values
Source Locations	$(z,z_s)=(0,70)$m
Receiver Locations	$(r,r_s)=(1000,20)$m
Water depth	80m

Sound velocity	1500 m/s
Salinity	35ppt
Water Temperature	14(degree Celsius)
Bottom type	bt = 1 (core sand) With mean grain size is 0.5 and roughness Is 1.85cm
Wind speed	Vw=8
pH	8

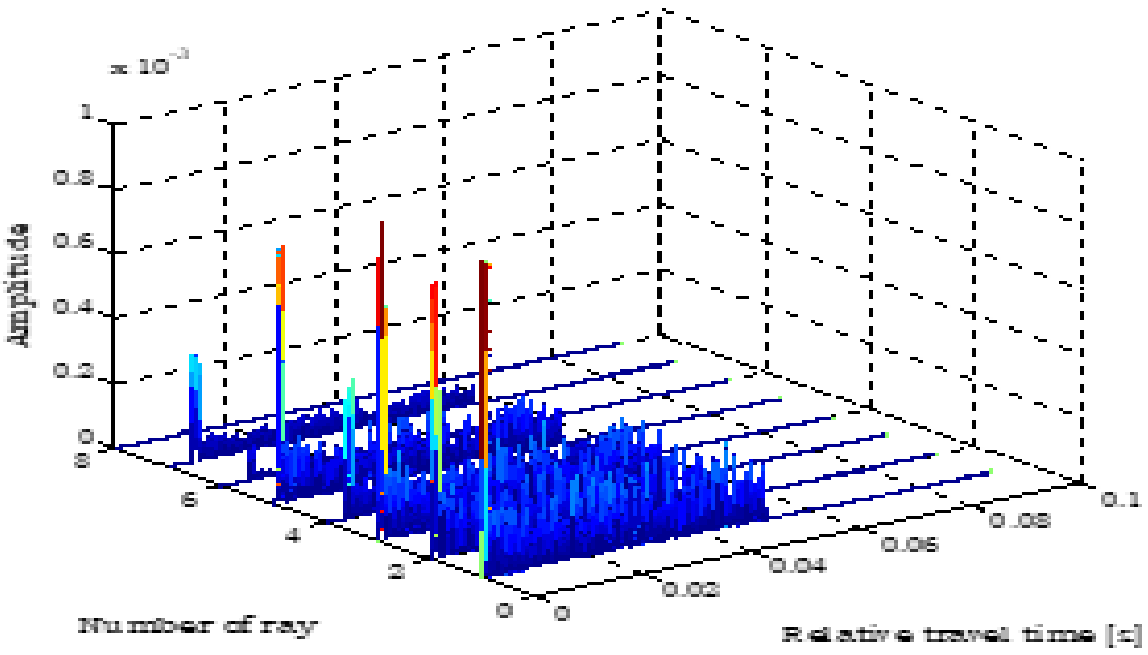

Figure 5.4. (Z,Z_S) = (0,70) and ((R,R_S) = (1000,20)

Simulation results showing relative travel times for various transmitter and receiver locations of a sine pulse including the transmission loss phenomenon for the scenarios.

TABLE 5.5. Time of arrival of different received paths for various transmitter and locations.

Source Location(m)	Receiver Location(m)	T_{01} (ms)	T_{02} (ms)	T_{03} (ms)	T_{04} (ms)	T_{11} (ms)	T_{12} (ms)	T_{13} (ms)	T_{14} (ms)
(0,20)	(100,70)	0.0745	0.0897	0.0814	0.0991	0.1551	0.1795	0.1672	0.1919
(0,70)	(100,20)	0.0745	0.0897	0.0814	0.6707	0.6812	0.1795	0.1672	0.2555
(0,20)	(1000,70)	0.6675	0.6694	0.6683	0.6707	0.6812	0.6872	0.6841	0.6905
(0,70)	(1000,20)	0.6675	0.6694	0.6683	0.6812	0.6707	0.6782	0.6841	0.7108

TABLE 5.6. Relative travel time of different received paths for various transmitter and locations

Source Location(m)	Receiver Location(m)	P_{01} (m)	P_{02} (m)	P_{03} (m)	P_{04} (m)	P_{11} (m)	P_{12} (m)	P_{13} (m)	P_{14} (m)
(0,20)	(100,70)	111.80	134.53	122.06	148.66	232.59	269.25	250.79	143.66
(0,70)	(100,20)	111.80	134.53	122.06	232.59	148.66	269.25	250.79	383.27
(0,20)	(1000,70)	1001.2	1004.0	1002.4	1.0060	1.0218	1.0308	1.0261	1.0358
(0,70)	(1000,20)	1001.2	1004.0	1002.4	1021.3	1006.0	1030.8	1023.1	1056.3

TABLE 5.7. the higher and lower grazing angles are observed due to shorter distances and larger distances between transmitter and receiver respectively. At lower grazing angles, the bottom reflection strength is higher, so that the effect of multipath is maximum

Source Location(m)	Receiver Location(m)	$\emptyset_{01}$ (degrees)	$\emptyset_{02}$ (degree	$\emptyset_{03}$ (degrees)	$\emptyset_{04}$ (degrees)	$\emptyset_{05}$ (degree	$\emptyset_{06}$ (degrees)	$\emptyset_{07}$ (degrees)	$\emptyset_{08}$ (degrees)
(0,20)	(100,70)	0.4636	0.7328	0.6107	0.833	1.126	1.190	1.160	1.216
(0,70)	(100,20)	0.4636	0.7328	0.6107	1.1264	0.8330	1.1903	1.1607	1.3068
(0,20)	(1000,70)	0.050	0.089	0.069	0.109	0.207	0.245	0.226	0.263

(0,70)	(1000,20)	-0.050	0.089	0.069	0.207	0.109	0.245	0.226	0.263

5.3 Communication System

BER plot analysis

QPSK BER Simulation over Multipath:

The first step is to determine the SNR value for the Quadrature Phase Shift Keying modulation technique, which has a lower BER value. Then, the system is modelled using these results, and it is shown that at 20 dB, the lowest BER is attained.

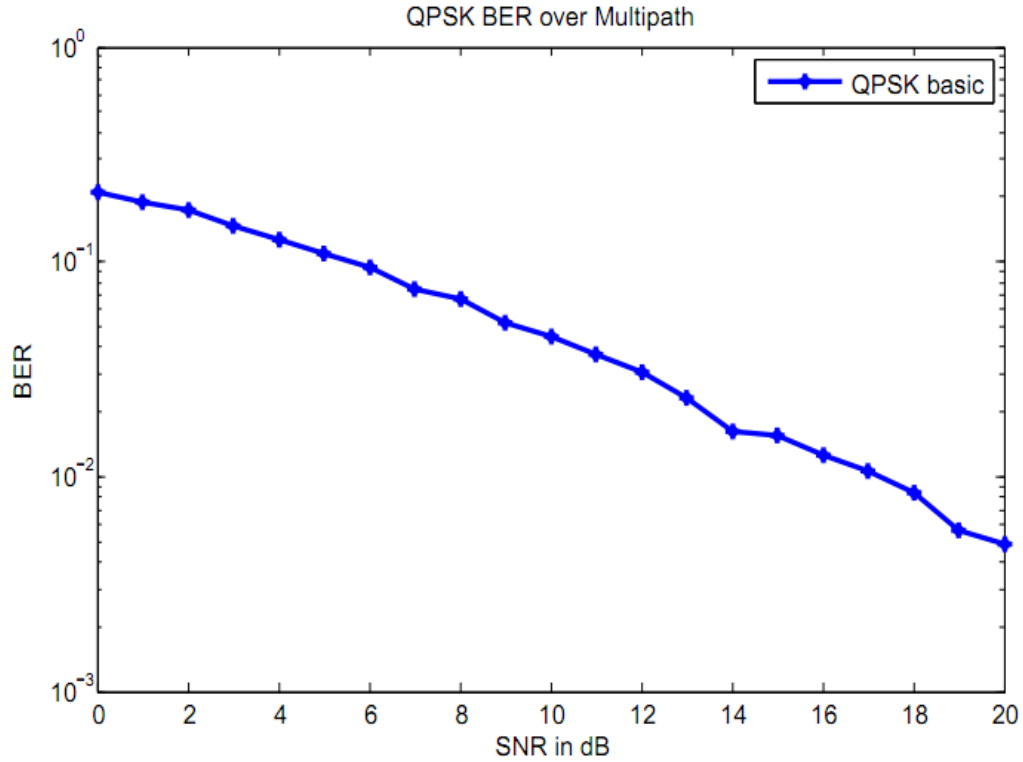

Figure 5.5. QPSK BER simulation in multipath

BER plot for QPSK by introducing Convolution Coding to the system over Multipath:

Similar to the previous section the convolution coding technique is added to the basic QPSK communication module over the multipath channel and the resulting BER plot from which one can interpret the improvement in BER in terms of SNR. The coding gain at 10^{-2} BER value is 8.23dB

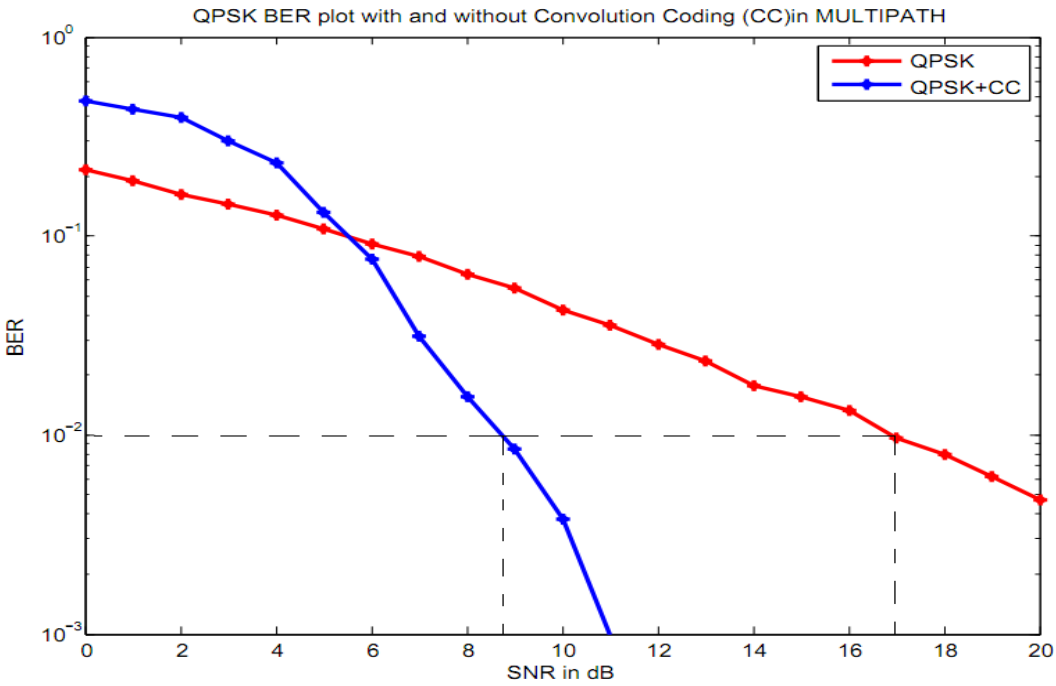

Figure 5.6. QPSK BER Simulation by introducing Convolution Coding in multipath.

BER plot for QPSK by applying both Convolution coding and pulse shaping filter to the basic QPSK system over Multipath.

It shows how the collective collaboration of convolution coding and pulse shaping helps in the improvement of BER performance in multipath transmission of data. It is observed that the result is nearly an analogy of transmitting the QPSK modulated data over WGN. At 10^{-2}BER the system gain is 6.43 dB.

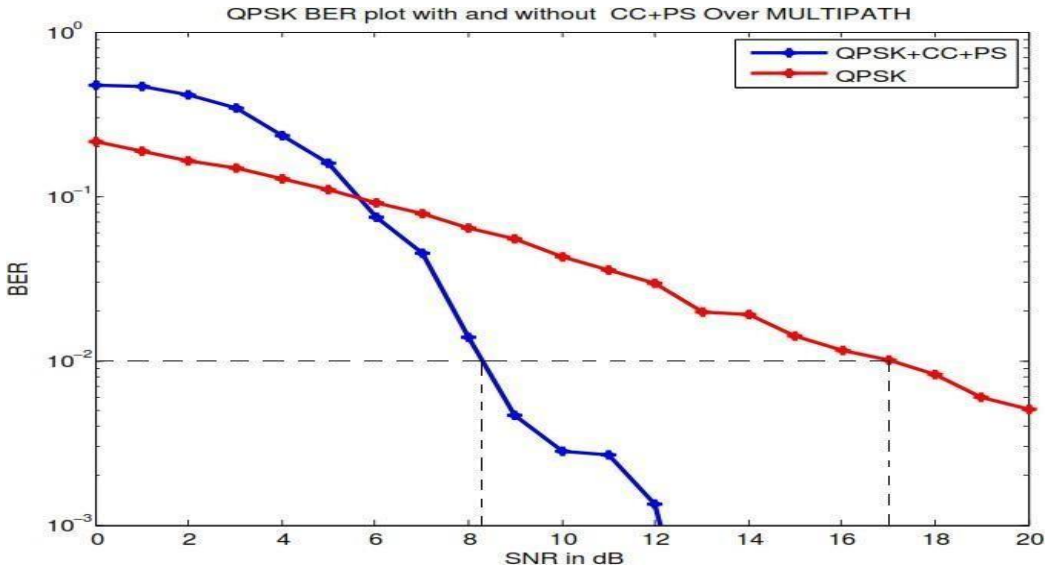

Figure 5.7. QPSK BER Simulation by introducing convolution coding and pulse shaping to the QPSKmodem in Multipath.

Maximum Likelihood Path :

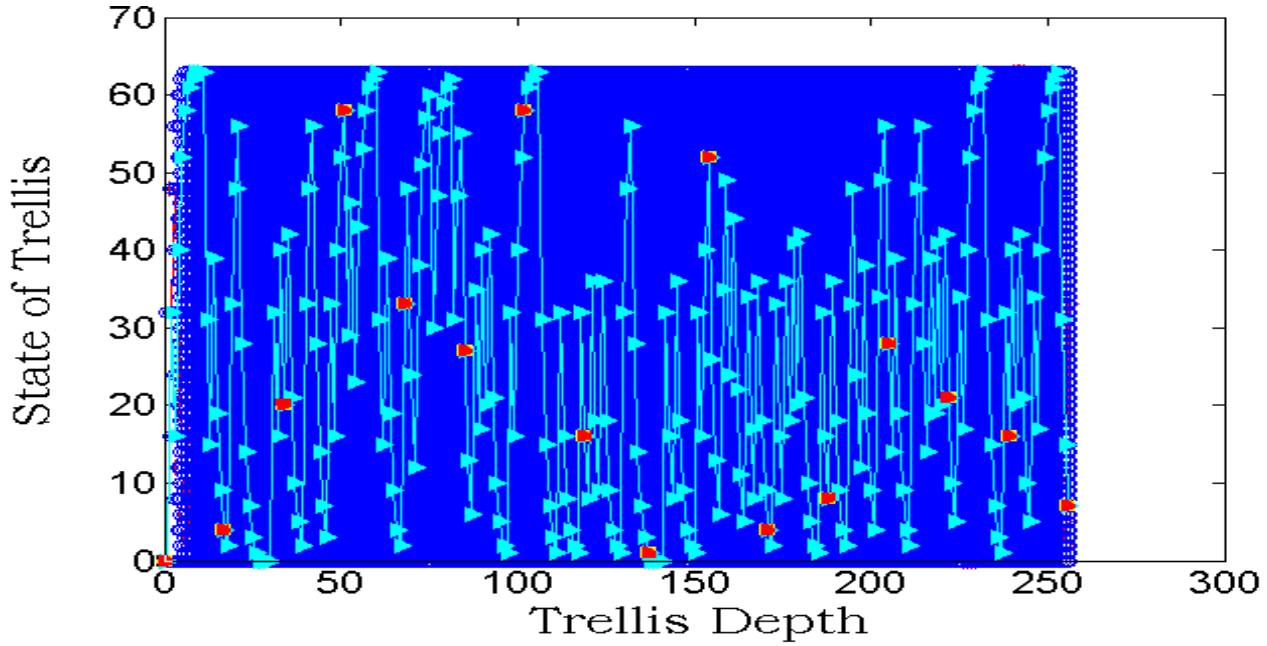

Figure 5.8 Maximum Likelihood Path for [0 1 1 0 0 0 0 1 0 1 1 0 0 0 1 0] message over multipath.

The fig 5.8 shows the decoded path for message signal over Multipath over Rayleigh Channel. It's clear from the fig that the decoded message is [0 1 0 0 1 0 1 1 0 0 1 1 0 0 1 0] when the actual message transmitted is [0 1 1 0 0 0 0 1 0 1 1 0 0 0 1 0].

CHAPTER 6

CONCLUSION AND FUTURE SCOPE

6. CONCLUSION AND FUTURE SCOPE

6.1. Conclusion

A mathematical model for the Shallow Under Water Acoustic communication channel is designed in this work.

First , it presented the multipath mathematical channel modelling for the shallow under water acoustic communication, considering the channel characteristics parameters from the actual environmental conditions of the sea.From the simulation results, it is observed that the multipath done as the range increases fro source to receiver.

Second, this work introduced single carrier QPSK system and from fig 6 without convolution coding the BER is 20 dB and after introducing the convolution coding it is observed from the fig 7. the BER improves at 8.23 dB.

6.2. Future Scope

As the channel variations gets worse the system's robustness gradually decreases due to interference (ISI) that destroys the message, because of different travel times for different rays. Hence, the future outlook for the extension of this system would be applying multi-modulation technique to improve the BER performance.

REFERENCES

[1] "A Ray-based Deep Learning Model for Shallow Water Acoustic Channel Estimation" by Rong Cheng, Chao Liang, and Jian Li. IEEE Journal of Oceanic Engineering, August 2022.

[2] "Spatiotemporal Statistical Properties of Underwater Acoustic Channels in a Shallow Sea Environment" by Haijiang Li, Shanshan Liang, and Jing Wang. IEEE Journal of Oceanic Engineering, May 2021.

[3] "Performance of Different Channel Estimation Techniques in a Shallow Water Acoustic Communication System" by Santhosh Kumar Gopalakrishnan, Nandhakumar Karuppusamy, and Subbiah Shanmugavel. IEEE Access, January 2022.

[4] "A Comparative Study of Underwater Acoustic Channel Estimation Techniques in a Shallow Water Environment" by Sana Khare, Suhaila S, and Sreedevi K Menon. Journal of Ambient Intelligence and Humanized Computing, March 2022.

[5] "An Improved Channel Estimation Method for Underwater Acoustic Communication Systems in Shallow Water Environments" by Mengxing Huang, Mingxi Wan, and Yanyan Chen. Sensors, September 2021.

[6]Underwater Acoustic Channel Modeling: Principles, Techniques, and Applications" by Yang Liu and Jian Li (2016).

[7]"Shallow Water Acoustics" by Robert J. Urick (1983).

[8]"Acoustic Propagation in Shallow Water: A Review" by A.D. Pierce (1992)